Articles

Multiplex, Quantitative, High-Resolution Imaging of Protein:Protein Complexes via Hybridization Chain Reaction

Samuel J. Schulte, Boyoung Shin, Ellen V. Rothenberg, and Niles A. Pierce*

Cite This: https://doi.org/10.1021/acschembio.3c00431
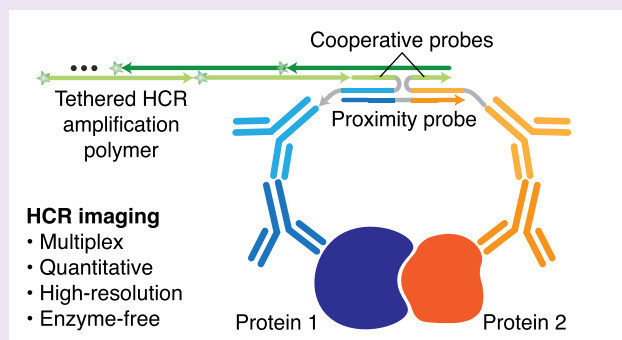
Read Online

ACCESS | Metrics & More | Article Recommendations | Supporting Information

ABSTRACT: Signal amplification based on the mechanism of hybridization chain reaction (HCR) facilitates spatial exploration of gene regulatory networks by enabling multiplex, quantitative, high-resolution imaging of RNA and protein targets. Here, we extend these capabilities to the imaging of protein:protein complexes, using proximity-dependent cooperative probes to conditionally generate a single amplified signal if and only if two target proteins are colocalized within the sample. HCR probes and amplifiers combine to provide automatic background suppression throughout the protocol, ensuring that even if reagents bind nonspecifically in the sample, they will not generate amplified background. We demonstrate protein:protein imaging with a high signal-to-background ratio in human cells, mouse proT cells, and highly autofluorescent formalin-fixed paraffin-embedded (FFPE) human breast tissue sections. Further, we demonstrate multiplex imaging of three different protein:protein complexes simultaneously and validate that HCR enables accurate and precise relative quantitation of protein:protein complexes with subcellular resolution in an anatomical context. Moreover, we establish a unified framework for simultaneous multiplex, quantitative, high-resolution imaging of RNA, protein, and protein:protein targets, with one-step, isothermal, enzyme-free HCR signal amplification performed for all target classes simultaneously.

INTRODUCTION

Methods for imaging molecular complexes[1,2] have been comparatively less explored than methods for imaging RNA and protein targets[3-8] yet represent an important frontier for spatial exploration of the interactome. Generating one signal conditional on the proximity of two molecules provides a subdiffraction-limit readout, in contrast to independent imaging of the same two molecules with two signals. Protein:protein complexes play central roles in diverse cellular processes including transcription, translation, signaling, development, and disease.[9-12] To date, imaging of protein:protein complexes has predominantly been performed using proximity ligation assays (PLA) that exploit enzyme-mediated ligation and rolling circle amplification,[13-17] leading to challenges with both false-negatives (formation of noncircular ligation products[17,18]) and false-positives (background evident in technical controls that omit one reaction component[17]), as well as issues with cost and variable enzyme activity.[13,17] Alternatively, to avoid the use of enzymes, a proximity-based HCR approach has been developed that uses a kinetic trigger mechanism to desequester an HCR initiator if two probes are bound to proximal target proteins;[18,19] this approach has so far been limited to 1-plex applications.

Over the course of nearly two decades, we have developed simple and robust HCR RNA fluorescence in situ hybrid-

ization (RNA-FISH) and immunofluorescence (IF) methods that enable biologists, drug developers, and pathologists to perform multiplex, quantitative, high-resolution imaging of RNA and protein targets in highly autofluorescent samples.[20-26] Here, we sought to use HCR principles to extend these benefits to the imaging of protein:protein complexes. An HCR amplifier consists of two species of kinetically trapped DNA hairpins (h1 and h2) that coexist metastably in solution, storing the energy to drive conditional self-assembly of an HCR amplification polymer upon exposure to a cognate initiator sequence (i1; Figure 1A).[27] Using HCR RNA-FISH, an RNA target is detected using one or more pairs of split-initiator DNA probes, each carrying a fraction of HCR initiator i1 (Figure 1B).[24] Probe pairs that hybridize specifically to proximal binding sites on the target RNA colocalize a full HCR initiator i1 capable of triggering HCR signal amplification. Meanwhile, any individual probes that bind nonspecifically in the sample do not colocalize full HCR
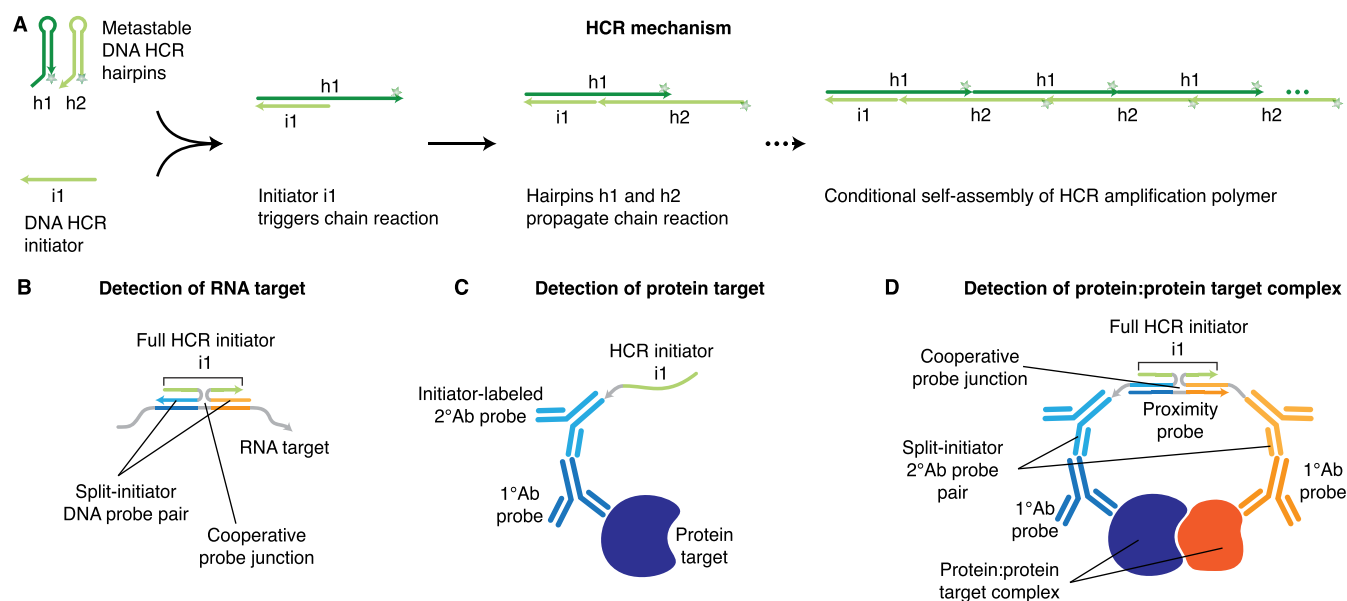
ACS Publications

A

Figure 1. Applying HCR principles to enable simple and robust imaging of protein:protein complexes. (A) HCR mechanism. Stars denote fluorophores. Arrowhead indicates the 3′ end of each strand. (B) HCR RNA-FISH: an RNA target is detected using a pair of split-initiator DNA probes, each carrying a fraction of HCR initiator i1. (C) HCR IF: a protein target is detected using an unlabeled primary antibody probe and an initiator-labeled secondary antibody probe carrying HCR initiator i1. (D) HCR protein:protein imaging: a protein:protein target complex is detected with a pair of unlabeled primary antibodies, a pair of split-initiator secondary antibodies each carrying a fraction of HCR initiator i1, and a proximity probe.
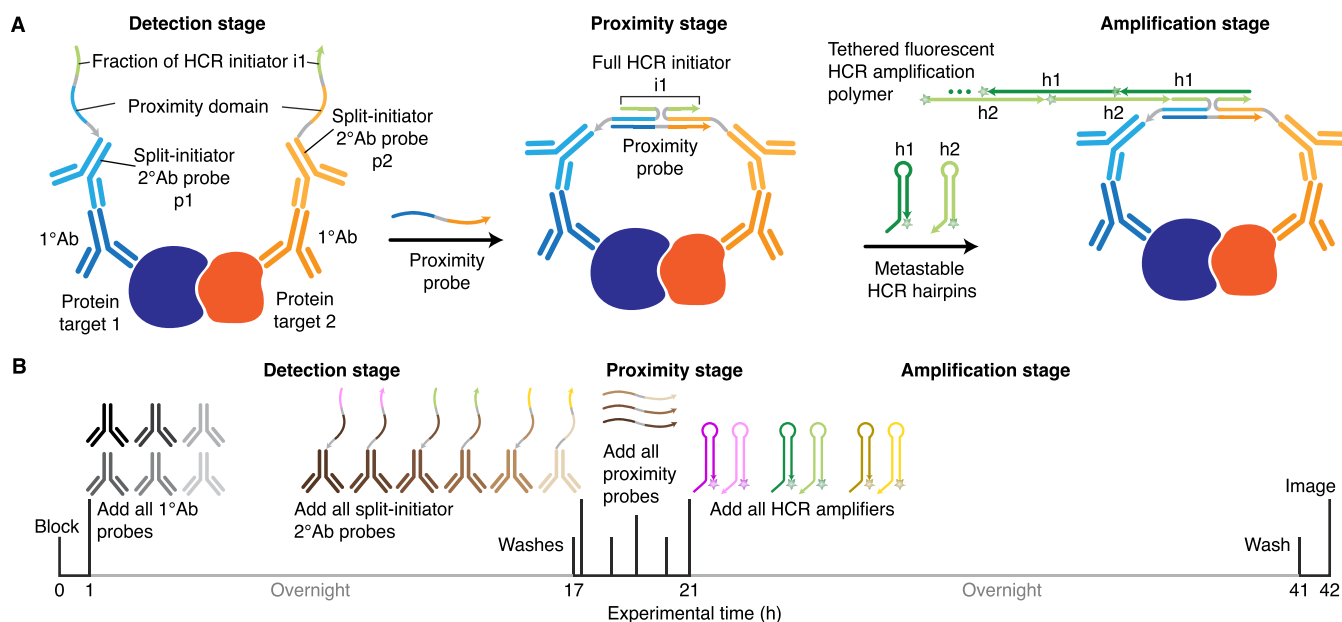

Figure 2. Imaging protein:protein complexes using HCR. (A) Three-stage protocol. Detection stage: unlabeled primary antibody probes bind to protein targets 1 and 2; wash; split-initiator secondary antibody probes p1 and p2 bind to primary antibody probes; wash. Proximity stage: if p1 and p2 are proximal, a proximity probe hybridizes to the proximity domains of p1 and p2 to colocalize full HCR initiator i1. Amplification stage: colocalized full HCR initiator i1 triggers self-assembly of fluorophore-labeled HCR hairpins into a tethered fluorescent amplification polymer; wash. (B) Multiplexing timeline. The same three-stage protocol is used independent of the number of protein:protein target complexes.

initiator i1 and do not trigger HCR. Using HCR IF, a protein target is detected using an unlabeled primary antibody probe, which in turn is detected by an initiator-labeled secondary antibody probe that carries an HCR initiator i1 capable of triggering HCR signal amplification (Figure 1C).[26]

We hypothesized that the split-initiator concept from HCR RNA-FISH (Figure 1B) could be generalized using the antibody probes of HCR IF (Figure 1C) to enable simple and robust HCR imaging of protein:protein complexes using a split-initiator antibody probe pair in conjunction with a new proximity probe (Figure 1D). Here, we demonstrate that this
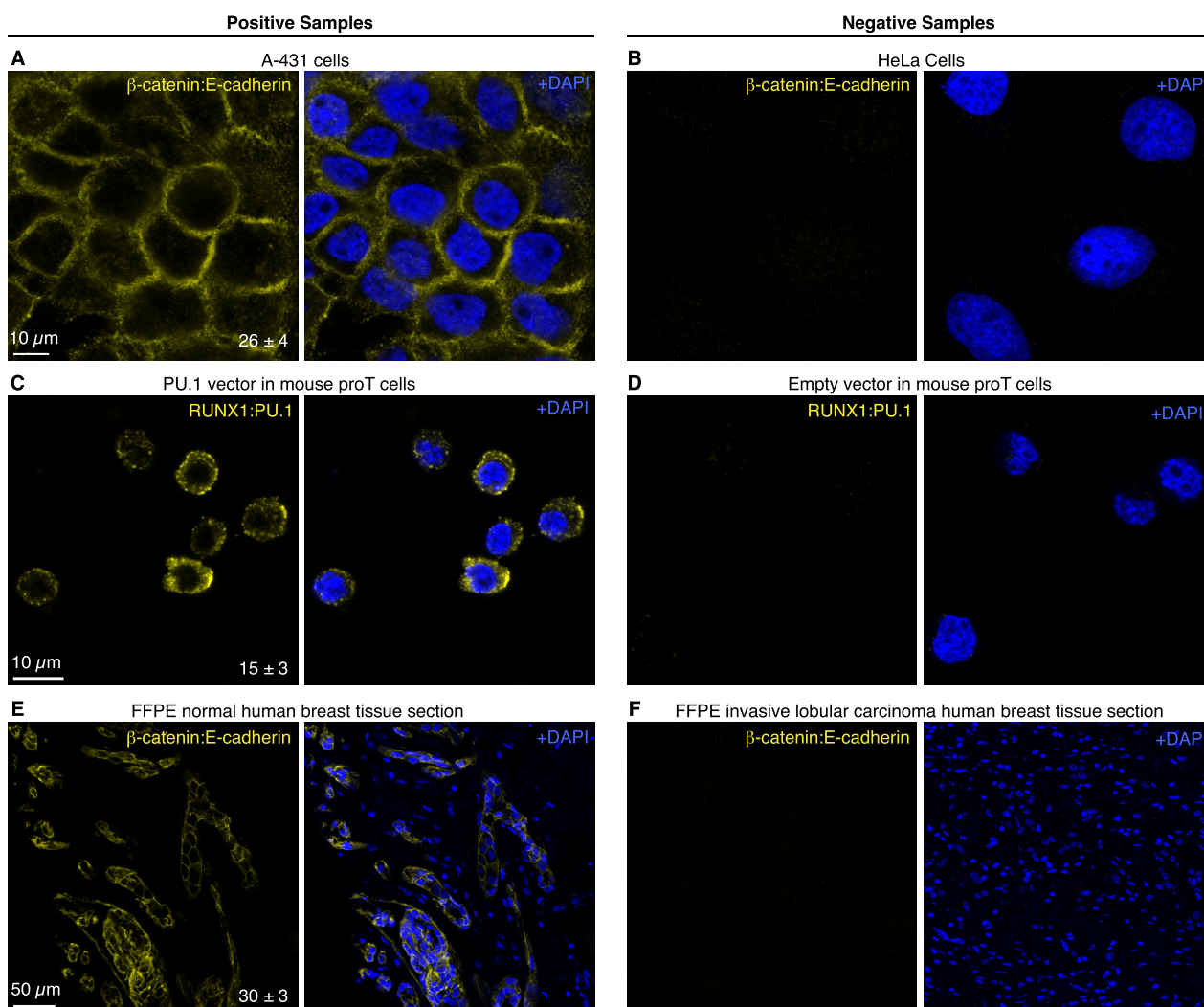
Figure 3. Imaging protein:protein complexes in human cells, mouse proT cells, and FFPE human breast tissue sections. (A,B) Imaging β-catenin:E-cadherin target complex in A-431 cells expressing β-catenin and E-cadherin (panel A) or HeLa cells expressing N-cadherin instead of E-cadherin (panel B). (C,D) Imaging RUNX1:PU.1 target complex in Scid.adh.2C2 mouse proT cells retrovirally transduced with a PU.1-expressing vector (panel C) or an empty vector (panel D). (E,F) Imaging β-catenin:E-cadherin target complex in 5 μm FFPE human breast tissue sections from the same patient: normal (panel E) or invasive lobular carcinoma (panel F). All panels: confocal image; single optical section; $0.18 \times 0.18 \times 0.8$ μm pixels (panels A–D) or $0.57 \times 0.57 \times 3.3$ μm pixels (panels E,F). Signal-to-backround ratio for each row (mean $\pm$ SEM for representative regions of $N = 3$ replicate samples). See sections S2.2–S2.4 for additional data.

combination of proximity-dependent cooperative probes and metastable HCR amplifiers enables multiplex, quantitative, high-resolution imaging of protein:protein complexes, including full compatibility with HCR RNA-FISH and HCR IF.

■ RESULTS AND DISCUSSION

HCR Imaging of Protein:Protein Complexes Using a Three-Stage Protocol. HCR imaging of protein:protein complexes is performed using the three-stage protocol summarized in Figure 2A. In the detection stage, two protein targets are detected with unlabeled primary antibody probes that are in turn detected by a pair of split-initiator secondary antibody probes (p1 and p2) each carrying a fraction of HCR initiator i1 and a proximity domain. In the proximity stage, if the two protein targets are colocalized in the sample, then the proximity probe is able to hybridize to p1 and p2 to colocalize a full HCR initiator i1 capable of triggering HCR signal amplification. Note that the proximity probe creates a

cooperative probe junction (Figure 1D) inspired by the cooperative probe junction created in HCR RNA-FISH (Figure 1B), with the DNA proximity probe taking the place of the RNA target. Any split-initiator probes that bind nonspecifically or to isolated protein targets in the sample can hybridize to the proximity probe but will not colocalize a full HCR initiator i1 and will not trigger HCR. In the amplification stage, each colocalized full HCR initiator i1 triggers self-assembly of metastable fluorophore-labeled HCR hairpins (h1 and h2) into a tethered fluorescent amplification polymer to generate an amplified signal at the site of the protein:protein target complex.

Imaging Protein:Protein Complexes in Human Cells, Mouse proT Cells, and FFPE Human Breast Tissue Sections. To evaluate the performance of our split-initiator approach for imaging protein:protein complexes, we compared the fluorescence intensity between three pairs of biological sample types using the same imaging settings for both sample types. Positive samples are expected to form the
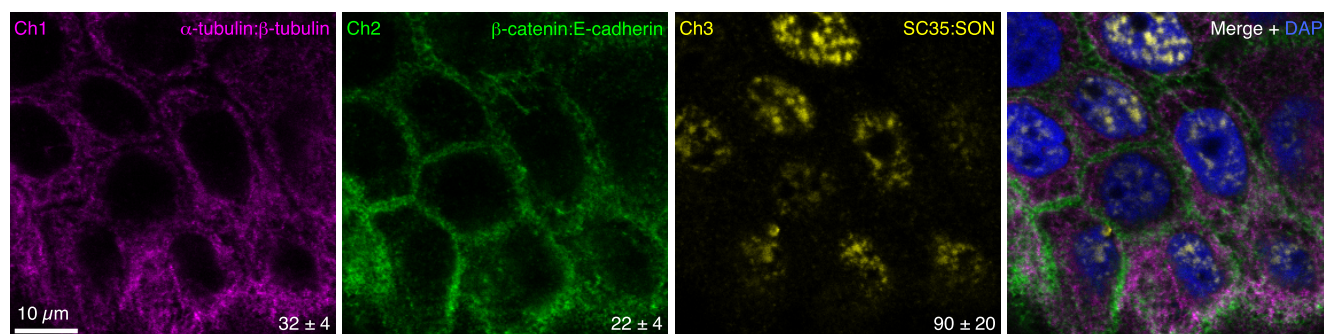
Figure 4. Multiplex imaging of protein:protein complexes. Three-channel confocal image in A-431 cells; single optical section; 0.18 × 0.18 × 0.8 μm pixels. Ch1: cytoskeletal α-tubulin:β-tubulin complex (Alexa488). Ch2: membranous β-catenin:E-cadherin complex (Alexa546). Ch3: nuclear speckle SC35:SON complex (Alexa647). Signal-to-background ratio for each channel (mean ± SEM for representative regions of N = 3 replicate wells on a slide). See section S2.5 for additional data.

protein:protein complex of interest; negative samples are expected to have minimal or no formation of the protein:protein complex of interest. For each pair of sample types, we calculate an estimated signal-to-background ratio using the positive sample type to estimate signal plus background and the negative sample type to estimate background. This approach yields a conservative estimate of performance, as characterizing background in a sample containing little or no protein:protein target complex places an upper bound on background and hence a lower bound on the signal-to-background ratio.

First, we compared the fluorescence intensity for the β-catenin:E-cadherin complex in A-431 and HeLa adherent human cell lines. While A-431 cells form the β-catenin:E-cadherin complex at the cell membrane of intercellular junctions,[28] HeLa cells express N-cadherin rather than E-cadherin[29,30] and therefore lack the β-catenin:E-cadherin complex. As expected, A-431 cells (Figure 3A) display a strong signal at intercellular junctions and HeLa cells display no visible staining (Figure 3B), with a signal-to-background ratio of 26 ± 4 between the two cell lines (mean ± SEM for representative regions of N = 3 replicate wells on a slide).

Next, we imaged Scid.adh.2C2[31] mouse proT cells in search of the RUNX1:PU.1 target complex. The Scid.adh.2C2 cell line has emerged as a useful proT cell line for studying T cell development, with exogenous introduction of PU.1 protein capable of reverting the cell line to an earlier developmental time point, in part via direct or indirect interactions between PU.1 and other proteins such as RUNX1.[32−34] Because the Scid.adh.2C2 cell line does not endogenously express the PU.1 protein,[31] Scid.adh.2C2 cells cannot natively form the RUNX1:PU.1 complex. When the Scid.adh.2C2 cell line is retrovirally transduced with PU.1, it is unknown whether PU.1 forms a complex with RUNX1 or interacts less directly.[33] Here, imaging the RUNX1:PU.1 target complex, we observe signal in cells retrovirally transduced with a PU.1-containing vector (Figure 3C) and no visible staining for cells retrovirally transduced with an empty vector (Figure 3D), with a signal-to-background ratio of 15 ± 3 between the two experiment types (mean ± SEM for representative regions of N = 3 replicate wells on a slide). These results provide evidence that RUNX1 and PU.1 are spatially colocalized in PU.1-transduced Scid.adh.2C2 cells and are not merely logically linked.

To test performance in highly autofluorescent samples, we detected the β-catenin:E-cadherin complex in normal and pathological FFPE human breast tissue sections. The β-catenin:E-cadherin complex is robustly formed in normal breast epithelial cells, but the expression of and interaction between the β-catenin and E-cadherin proteins is interrupted when breast epithelial cells become cancerous in the invasive lobular carcinoma disease process.[35,36] We obtained paired normal and invasive lobular carcinoma FFPE breast tissue sections from the same patient and evaluated them for the β-catenin:E-cadherin complex, observing a strong signal in normal breast tissue (Figure 3E) and no visible staining in cancerous tissue (Figure 3F), with a signal-to-background ratio of 30 ± 3 between the two tissue types (mean ± SEM for representative regions of N = 3 replicate sections).

In summary, protein:protein complexes are imaged with high signal-to-background across three different paired sample types, including highly autofluorescent FFPE tissues.

Multiplex Protein:Protein Imaging. HCR RNA-FISH and HCR IF enable straightforward multiplexing for RNA and protein targets to allow multidimensional analyses of gene expression in an anatomical context.[20−22,24−26] To likewise enable multiplex imaging of protein:protein complexes, we used NUPACK[37,38] to design proximity probes for three orthogonal HCR amplifiers. Figure 4 demonstrates multiplex protein imaging for three target complexes that localize to different compartments of A-431 adherent human cells: cytoskeletal α-tubulin:β-tubulin complex, membranous β-catenin:E-cadherin complex, and nuclear speckle SC35:SON complex. High signal-to-background is observed for all three protein:protein target complexes, with background estimated based on technical control experiments that omit the primary and secondary antibody probes for one protein or the other within a given complex (see Table S13 for details). Multiplexing is straightforward using a three-stage protocol independent of the number of protein:protein target complexes (Figure 2B): all protein targets are detected in parallel, proximity is verified for all protein target pairs in parallel, and amplification is performed for all colocalized full HCR initiators in parallel.

qHCR Imaging: Relative Quantitation of Protein:Protein Complexes with Subcellular Resolution. We have previously demonstrated that HCR imaging enables accurate and precise relative quantitation of both RNA and protein targets with subcellular resolution in an anatomical context, generating an amplified signal that scales approximately linearly with the number of target molecules per imaging voxel.[24−26] Here, we validate that the proximity
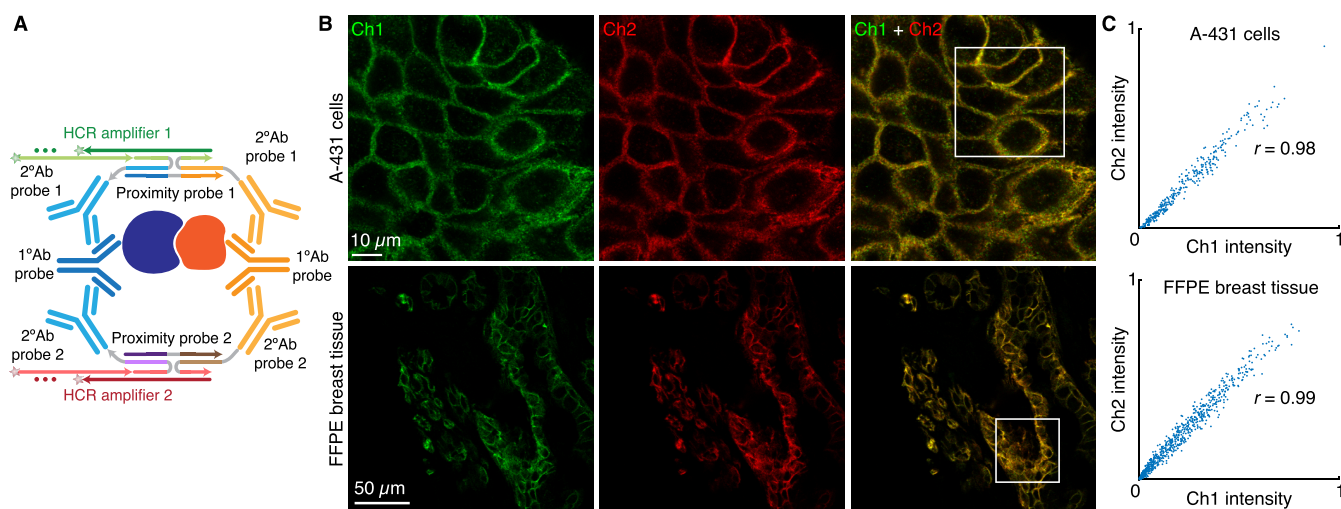
Figure 5. qHCR imaging: relative quantitation of protein:protein complexes with subcellular resolution in an anatomical context. (A) Two-channel redundant detection of a protein:protein complex: each target protein is detected by an unlabeled primary antibody probe and two batches of secondary antibody probes that interact with orthogonal proximity probes to colocalize full HCR initiators that trigger orthogonal spectrally distinct HCR amplifiers (Ch1, Alexa546; Ch2, Alexa647). (B) Two-channel confocal images; single optical sections. Top: β-catenin:E-cadherin complex in A-431 cells ($0.18 \times 0.18 \times 0.8 \ \mu$m pixels). Bottom: β-catenin:E-cadherin complex in a 5 μm FFPE normal human breast tissue section ($0.57 \times 0.57 \times 3.3 \ \mu$m pixels). (C) High accuracy and precision for protein:protein relative quantitation in an anatomical context. Highly correlated normalized signal (Pearson correlation coefficient, r) for subcellular voxels in the indicated regions in panel B. Top: $2.0 \times 2.0 \times 0.8 \ \mu$m voxels. Bottom: $2.0 \times 2.0 \times 3.3 \ \mu$m voxels. Accuracy: linearity with zero intercept. Precision: scatter around the line. See section S2.6 for additional data.

probe and split-initiator antibody probe pair preserve the quantitative nature of HCR imaging for protein:protein target complexes. To test relative quantitation, we detect each protein in the complex with an unlabeled primary antibody probe as usual and then redundantly detect each primary antibody probe with two batches of split-initiator secondary antibody probes, where each batch interacts with a different proximity probe and triggers a different spectrally distinct HCR amplifier (Figure 5A), yielding a two-channel image (Figure 5B). If HCR signal scales approximately linearly with the number of target protein:protein complexes per voxel, a two-channel scatter plot of normalized voxel intensities will yield a tight linear distribution with zero intercept.[25] Consistent with expectation, we observe high accuracy (linearity with zero intercept) and precision (scatter around the line) for subcellular voxels in both cultured human cells (Figure 5C; top) and highly autofluorescent FFPE human breast tissue (Figure 5C; bottom).

Simultaneous Multiplex Imaging of Protein, Protein:Protein, and RNA Targets. We have previously shown that HCR RNA-FISH and HCR IF enable multiplex, quantitative, high-resolution RNA and protein imaging in highly autofluorescent samples.[26] Here, we demonstrate compatible multiplex imaging of protein, protein:protein, and RNA targets using initiator-labeled antibody probes for protein targets, proximity probes and split-initiator antibody probe pairs for protein:protein targets, and split-initiator DNA probe pairs for RNA targets with simultaneous HCR signal amplification for all target classes (Figure 6A). In A-431 adherent human cells, mitochondrial HSP60 protein targets, cytoskeletal α-tubulin:β-tubulin protein:protein target complexes, and nuclear U6 RNA targets are all imaged simultaneously (Figure 6B) with high signal-to-background (see Table S18 for additional details).

Unified Framework for Multiplex, Quantitative, High-Resolution Imaging. We have shown that HCR imaging provides a unified framework for multiplex, quantitative, high-resolution imaging of RNA targets, protein targets, and protein:protein target complexes simultaneously. A high signal-to-background ratio is achieved even in highly autofluorescent samples. As a natural property of this method, the amplified signal scales approximately linearly with target abundance, enabling accurate and precise relative quantitation of each target with subcellular resolution in an anatomical context. By contrast, the amplified signal using PLA methods does not scale linearly with target abundance.[16] Using the validated proximity probes presented here, up to three protein:protein target complexes can be imaged simultaneously, in combination with RNA or protein targets of choice. Multiplex HCR protein:protein imaging is achieved using a three-stage protocol (detection stage, proximity stage, and amplification stage) involving two overnight incubations. Simultaneous multiplex imaging of protein, protein:protein, and RNA targets is achieved using a four-stage protocol (protein detection stage, proximity stage, RNA detection stage, and amplification stage) involving three overnight incubations. The use of overnight incubations reflects our longstanding focus on developing versatile protocols that are suitable for diverse sample types including whole-mount vertebrate embryos while allowing researchers to maintain a normal sleep schedule.[20,21,24,26] If desired, HCR imaging protocols can be optimized to use shorter incubation times in sample types of interest.[39−41]

Automatic Background Suppression Throughout the Protocol. As is the case for HCR RNA-FISH, the use of split-initiator probes during the detection stage and metastable HCR hairpins during the amplification stage provides automatic background suppression throughout the protocol, ensuring that even if reagents bind nonspecifically
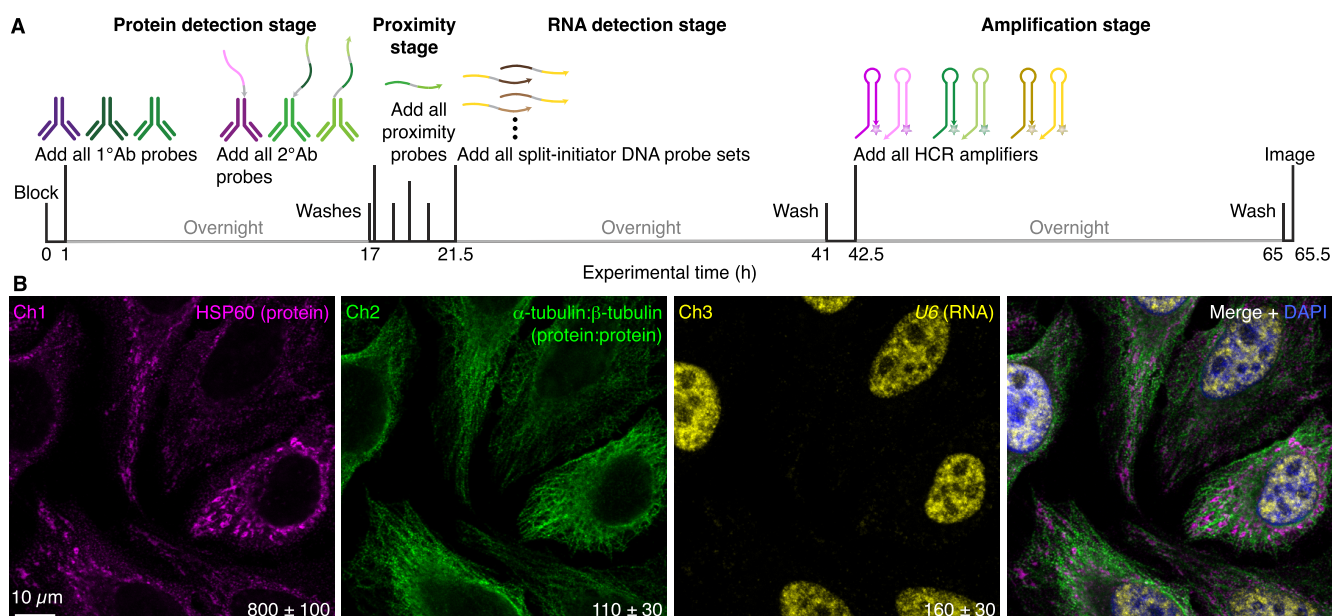
Figure 6. Simultaneous multiplex protein, protein:protein, and RNA imaging using HCR. (A) Four-stage protocol. Protein detection stage: unlabeled primary antibody probes bind to protein targets; wash; secondary antibody probes bind to primary antibody probes (initiator-labeled 2°Ab probes associated with individual protein targets carry full initiators; split-initiator 2°Ab probes associated with protein:protein target complexes carry a fraction of HCR initiator i1 and a proximity domain); wash. Proximity stage: proximity probes colocalize a full HCR initiator i1 for protein:protein target complexes; wash. RNA detection stage: split-initiator DNA probes bind to RNA targets; wash. Amplification stage: initiators trigger self-assembly of fluorophore-labeled HCR hairpins into tethered fluorescent HCR amplification polymers; wash. (B) Three-channel confocal image in HeLa cells; single optical section; $0.18 \times 0.18 \times 0.8$ μm pixels. Ch1: mitochondrial HSP60 protein (Alexa488). Ch2: cytoskeletal α-tubulin:β-tubulin complex (Alexa546). Ch3: nuclear U6 RNA (Alexa647). Signal-to-background ratio for each channel (mean ± SEM for representative regions of N = 3 replicate wells on a slide). See section S2.7 for additional data.

in the sample, they do not generate amplified background.[24] During the detection stage, any individual probes that bind nonspecifically in the sample do not colocalize a full HCR initiator and do not trigger HCR. Likewise, during the proximity stage for protein:protein imaging, any proximity probes that bind nonspecifically in the sample lack the ability to initiate HCR. During the amplification stage, any HCR hairpins that bind nonspecifically in the sample are kinetically trapped and do not trigger formation of an HCR amplification polymer. Automatic background suppression enhances the signal-to-background ratio and quantitative accuracy and precision.[24]

Split-Initiator Primary Antibody Probes vs Split-Initiator Secondary Antibody Probes. The work presented here employs unlabeled primary antibody probes and split-initiator secondary antibody probes to detect protein:protein complexes, thereby requiring that each primary antibody be of a different isotype or raised in a different host species. Given the large libraries of commercial antibodies available to users, this requirement is often not an impediment. For example, to image three protein:protein complexes simultaneously (Figure 4), we employ chicken IgY, mouse IgG1, mouse IgG2a, mouse IgG2b, guinea pig IgG, and rabbit IgG primary antibody probes to detect the six target proteins. However, when it is desirable to use multiple primary antibodies raised in the same host species or of the same isotype, just as HCR IF can be performed using initiator-labeled primary antibody probes,[26] there is the option to perform HCR protein:protein imaging using split-initiator primary antibody probes (see the diagrams of Figure S1). Because antibody-oligo conjugation can sometimes interfere with target recognition, there is a practical advantage

to using split-initiator secondary antibody probes, as we do here: using a small library of validated split-initiator secondary antibody probes, users can plug-and-play with large libraries of unmodified primary antibody probes with no need to validate antibody-oligo conjugation for each new target protein. Additionally, because multiple split-initiator secondary antibody probes can bind to each primary antibody probe, there is the potential for proximity probes to colocalize multiple full HCR initiators per target complex, triggering growth of multiple tethered fluorescent amplification polymers and increasing amplification gain and quantitative precision (note that with qHCR imaging, quantitative precision increases with probe set size[25]).

Subdiffraction-Limit Worst-Case Bound on Resolution of Signal Generation. The spatial resolution of three-dimensional fluorescence images is diffraction-limited to ~200 nm in lateral directions and to ~500 nm in the axial direction.[42,43] Using HCR to image a pair of colocalized target proteins, an amplified HCR signal is generated if the two protein targets are sufficiently close together that the proximity probe is able to bind split-initiator secondary antibody probes p1 and p2 to colocalize a full HCR initiator. A worst-case upper bound on the resolution of signal generation is obtained by stretching all of the probes out linearly (two unlabeled primary antibody probes, two split-initiator secondary antibody probes, and a proximity probe) to maximize the distance between the two protein targets (Figure S2). Estimating the extent of each antibody as 12.5 nm[44−46] and the extent of each oligonucleotide at 0.34 nm per base pair and 0.676 nm per unpaired base, the worst-case upper bound on the resolution of signal generation is 74 nm in both lateral and axial directions (well below diffraction-

limited resolution). In practice, it may not be feasible for the probes to adopt a linear arrangement, so the actual resolution for signal generation may be better than the worst-case bound. Note that commercial PLA methods employ two primary antibodies and two secondary antibodies as well as circularization oligonucleotides,[47] leading to a comparable worst-case bound on the resolution of signal generation using the above antibody and oligonucleotide dimensions. In future work on HCR protein:protein imaging, the resolution of signal generation could be enhanced by using split-initiator primary antibody probes and eliminating the use of secondary antibody probes, or by using nanobodies (4 nm extent[46]) in place of antibodies.

Simple, Robust, Enzyme-Free Imaging of Protein:-Protein Complexes. In conclusion, HCR principles[27] drawn from the emerging discipline of dynamic nucleic acid nanotechnology lead to an enzyme-free approach for imaging protein:protein complexes that retains the desirable simplicity and robustness of RNA and protein imaging using HCR RNA-FISH[24] and HCR IF.[26]

METHODS

Probes, Amplifiers, and Buffers. Probes, amplifiers, and buffers were obtained from Molecular Technologies, a nonprofit academic resource within the Beckman Institute at Caltech. Details on the probes, amplifiers, and buffers for each experiment are displayed in Table S1 for HCR imaging of protein:protein complexes, in Table S2 for HCR RNA-FISH, and in Table S3 for HCR IF.

HCR Imaging of Protein:Protein Complexes. HCR imaging of protein:protein complexes, with optional codetection of protein and RNA targets, was performed in adherent human cell lines (A-431 or HeLa) using the protocol detailed in section S1.9. A-431 cells (ATCC, CRL-1555) were cultured in Dulbecco's Modified Eagle Medium (DMEM) with high glucose and pyruvate (Gibco, 11995-073) supplemented with 10% fetal bovine serum (FBS; Sigma-Aldrich, F4135). HeLa cells (ATCC, CRM-CCL-2) were cultured in Eagle's Minimum Essential Medium (EMEM; ATCC, 30-2003) supplemented with 10% FBS (Sigma-Aldrich, F4135). HCR imaging of protein:protein complexes was performed in Scid.adh.2C2 mouse proT cells[31] cultured in RPMI1640 media (Gibco, 31800022) supplemented with 10% FBS (Sigma-Aldrich, F2442), 1× penicillin−streptomycin−glutamine (Gibco, 10378-016), 0.1 mM sodium pyruvate (Gibco, 11360-070), 1× MEM nonessential amino acids (Gibco, 11140−050), and 50 μM β-mercaptoethanol (Gibco, 21985-023) using the protocol detailed in section S1.10. HCR imaging of protein:protein complexes was performed in 5 μm FFPE normal human breast tissue sections (Acepix Biosciences, HuN-06-0027) and 5 μm FFPE invasive lobular carcinoma human breast tissue sections (Acepix Biosciences, HuC-06-0101) from the same patient using the protocol detailed in section S1.11.

Microscopy. Confocal microscopy was performed using a Leica Stellaris 8 inverted confocal microscope. All images are displayed without background subtraction. Each channel (except for DAPI) is displayed with 0.01% of the pixels saturated across three replicates. Details on the objectives, excitation wavelengths, detectors, and detection wavelengths used for each experiment are displayed in Table S5.

Image Analysis. Image analysis was performed as detailed in section S1.8, including the definition of raw pixel intensities; measurement of signal, background, and signal-to-background ratio; and calculation of normalized subcellular voxel intensities for qHCR imaging.

ASSOCIATED CONTENT

Ⓢ Supporting Information

The Supporting Information is available free of charge at https://pubs.acs.org/doi/10.1021/acschembio.3c00431.

> Materials, additional methods, protocols, and replicate data (PDF)

AUTHOR INFORMATION

Corresponding Author

  Niles A. Pierce − *Division of Biology and Biological Engineering, California Institute of Technology, Pasadena, California 91125, United States; Division of Engineering and Applied Science, California Institute of Technology, Pasadena, California 91125, United States;* Ⓞ orcid.org/0000-0003-2367-4406; Email: niles@caltech.edu

Authors

  Samuel J. Schulte − *Division of Biology and Biological Engineering, California Institute of Technology, Pasadena, California 91125, United States*

  Boyoung Shin − *Division of Biology and Biological Engineering, California Institute of Technology, Pasadena, California 91125, United States*

  Ellen V. Rothenberg − *Division of Biology and Biological Engineering, California Institute of Technology, Pasadena, California 91125, United States*

Complete contact information is available at:
https://pubs.acs.org/10.1021/acschembio.3c00431

Notes

The authors declare the following competing financial interest(s): Patents, pending patent applications, and the startup company Molecular Instruments.

ABBREVIATIONS

FFPE, formalin-fixed paraffin-embedded; HCR, hybridization chain reaction; IF, immunofluorescence; FISH, fluorescence in situ hybridization; PLA, proximity ligation assay; qHCR, quantitative hybridization chain reaction.

REFERENCES

(1) Söderberg, O.; Leuchowius, K.-J.; Gullberg, M.; Jarvius, M.; Weibrecht, I.; Larsson, L.-G.; Landegren, U. Characterizing proteins and their interactions in cells and tissues using the in situ proximity ligation assay. *Methods* **2008**, *45*, 227−232.

(2) Greenwood, C.; Ruff, D.; Kirvell, S.; Johnson, G.; Dhillon, H. S.; Bustin, S. A. Proximity assays for sensitive quantification of proteins. *Biomol. Detect. Quantif.* **2015**, *4*, 10−16.

(3) Coons, A. H.; Creech, H. J.; Jones, R. N. Immunological properties of an antibody containing a fluorescent group. *Proc. Soc. Exp. Biol. Med.* **1941**, *47* (2), 200−202.

(4) Harrison, P. R.; Conkie, D.; Paul, J.; Jones, K. Localisation of cellular globin messenger RNA by in situ hybridisation to complementary DNA. *FEBS Lett.* **1973**, *32* (1), 109−112.

(5) Tautz, D.; Pfeifle, C. A non-radioactive in situ hybridization method for the localization of specific RNAs in *Drosophila* embryos reveals translational control of the segmentation gene hunchback. *Chromosoma* **1989**, *98*, 81−85.

(6) Qian, X.; Jin, L.; Lloyd, R. V. In situ hybridization: Basic approaches and recent development. *J. Histotechnol.* **2004**, *27* (1), 53−67.

(7) Ramos-Vara, J. A. Technical aspects of immunohistochemistry. *Vet. Pathol.* **2005**, *42*, 405−426.

(8) Kim, S.-W.; Roh, J.; Park, C.-S. Immunohistochemistry for pathologists: Protocols, pitfalls, and tips. *J. Pathol. Transl. Med.* **2016**, *50* (6), 411−418.

(9) Braun, P.; Gingras, A.-C. History of protein-protein interactions: From egg-white to complex networks. *Proteomics* **2012**, *12* (10), 1478−1498.

(10) Sahni, N.; Yi, S.; Taipale, M.; Fuxman Bass, J. I.; Coulombe-Huntington, J.; Yang, F.; Peng, J.; Weile, J.; Karras, G. I.; Wang, Y.; Kovács, I. A.; Kamburov, A.; Krykbaeva, I.; Lam, M. H.; Tucker, G.; Khurana, V.; Sharma, A.; Liu, Y.-Y.; Yachie, N.; Zhong, Q.; Shen, Y.; Palagi, A.; San-Miguel, A.; Fan, C.; Balcha, D.; Dricot, A.; Jordan, D. M.; Walsh, J. M.; Shah, A. A.; Yang, X.; Stoyanova, A. K.; Leighton, A.; Calderwood, M. A.; Jacob, Y.; Cusick, M. E.; Salehi-Ashtiani, K.; Whitesell, L. J.; Sunyaev, S.; Berger, B.; Barabási, A.-L.; Charloteaux, B.; Hill, D. E.; Hao, T.; Roth, F. P.; Xia, Y.; Walhout, A. J. M.; Lindquist, S.; Vidal, M. Widespread macromolecular interaction perturbations in human genetic disorders. *Cell* **2015**, *161* (3), 647−660.

(11) Mei, S.; Zhu, H. A simple feature construction method for predicting upstream/downstream signal flow in human protein-protein interaction networks. *Sci. Rep* **2015**, *5* (1), 17983.

(12) Murakami, Y.; Tripathi, L. P.; Prathipati, P.; Mizuguchi, K. Network analysis and in silico prediction of protein−protein interactions with applications in drug discovery. *Curr. Opin. Struct. Biol.* **2017**, *44*, 134−142.

(13) Söderberg, O.; Gullberg, M.; Jarvius, M.; Ridderstrale, K.; Leuchowius, K. J.; Jarvius, J.; Wester, K.; Hydbring, P.; Bahram, F.; Larsson, L. G.; Landegren, U. Direct observation of individual endogenous protein complexes in situ by proximity ligation. *Nat. Methods* **2006**, *3* (12), 995−1000.

(14) Leuchowius, K. J.; Clausson, C. M.; Grannas, K.; Erbilgin, Y.; Botling, J.; Zieba, A.; Landegren, U.; Söderberg, O. Parallel visualization of multiple protein complexes in individual cells in tumor tissue. *Mol. Cell. Proteomics* **2013**, *12* (6), 1563−71.

(15) Bellucci, A.; Fiorentini, C.; Zaltieri, M.; Missale, C.; Spano, P. The in situ proximity ligation assay to probe protein-protein interactions in intact tissues. *Methods Mol. Biol.* **2014**, *1174*, 397−405.

(16) Koos, B.; Andersson, L.; Clausson, C. M.; Grannas, K.; Klaesson, A.; Cane, G.; Söderberg, O. Analysis of protein interactions in situ by proximity ligation assays. *Curr. Top. Microbiol. Immunol.* **2013**, *377*, 111−26.

(17) Klaesson, A.; Grannas, K.; Ebai, T.; Heldin, J.; Koos, B.; Leino, M.; Raykova, D.; Oelrich, J.; Arngården, L.; Söderberg, O.; Landegren, U. Improved efficiency of in situ protein analysis by proximity ligation using UnFold probes. *Sci. Rep* **2018**, *8* (1), 5400.

(18) Koos, B.; Cane, G.; Grannas, K.; Löf, L.; Arngården, L.; Heldin, J.; Clausson, C. M.; Klaesson, A.; Hirvonen, M. K.; de Oliveira, F. M. S.; Talibov, V. O.; Pham, N. T.; Auer, M.; Danielson, U. H.; Haybaeck, J.; Kamali-Moghaddam, M.; Söderberg, O.

(19) Leino, M.; Heldin, J.; Sander, M. R.; Kermpatsou, D.; Raykova, D.; Koos, B.; Söderberg, O. Optimization of proximity-dependent initiation of hybridization chain reaction for improved performance. *Mol. Syst. Des. Eng.* **2019**, *4* (5), 1058−1065.

(20) Choi, H. M. T.; Chang, J. Y.; Trinh, L. A.; Padilla, J. E.; Fraser, S. E.; Pierce, N. A. Programmable in situ amplification for multiplexed imaging of mRNA expression. *Nat. Biotechnol.* **2010**, *28* (11), 1208−12.

(21) Choi, H. M. T.; Beck, V. A.; Pierce, N. A. Next-generation in situ hybridization chain reaction: Higher gain, lower cost, greater durability. *ACS Nano* **2014**, *8* (5), 4284−4294.

(22) Choi, H. M. T.; Calvert, C. R.; Husain, N.; Huss, D.; Barsi, J. C.; Deverman, B. E.; Hunter, R. C.; Kato, M.; Lee, S. M.; Abelin, A. C. T.; Rosenthal, A. Z.; Akbari, O. S.; Li, Y.; Hay, B. A.; Sternberg, P. W.; Patterson, P. H.; Davidson, E. H.; Mazmanian, S. K.; Prober, D. A.; van de Rijn, M.; Leadbetter, J. R.; Newman, D. K.; Readhead, C.; Bronner, M. E.; Wold, B.; Lansford, R.; Sauka-Spengler, T.; Fraser, S. E.; Pierce, N. A. Mapping a multiplexed zoo of mRNA expression. *Development* **2016**, *143*, 3632−3637.

(23) Shah, S.; Lubeck, E.; Schwarzkopf, M.; He, T.-F.; Greenbaum, A.; Sohn, C. H.; Lignell, A.; Choi, H. M. T.; Gradinaru, V.; Pierce, N. A.; Cai, L. Single-molecule RNA detection at depth via hybridization chain reaction and tissue hydrogel embedding and clearing. *Development* **2016**, *143*, 2862−2867.

(24) Choi, H. M. T.; Schwarzkopf, M.; Fornace, M. E.; Acharya, A.; Artavanis, G.; Stegmaier, J.; Cunha, A.; Pierce, N. A. Third-generation in situ hybridization chain reaction: Multiplexed, quantitative, sensitive, versatile, robust. *Development* **2018**, *145*, dev165753.

(25) Trivedi, V.; Choi, H. M. T.; Fraser, S. E.; Pierce, N. A. Multidimensional quantitative analysis of mRNA expression within intact vertebrate embryos. *Development* **2018**, *145*, dev156869.

(26) Schwarzkopf, M.; Liu, M. C.; Schulte, S. J.; Ives, R.; Husain, N.; Choi, H. M. T.; Pierce, N. A. Hybridization chain reaction enables a unified approach to multiplexed, quantitative, high-resolution immunohistochemistry and in situ hybridization. *Development* **2021**, *148* (22), dev199847.

(27) Dirks, R. M.; Pierce, N. A. Triggered amplification by hybridization chain reaction. *Proc. Natl. Acad. Sci. U. S. A.* **2004**, *101* (43), 15275−15278.

(28) Chitaev, N. A.; Troyanovsky, S. M. Adhesive but not lateral E-cadherin complexes require calcium and catenins for their formation. *J. Cell Biol.* **1998**, *142* (3), 837−846.

(29) Wahl, J. K.; Kim, Y. J.; Cullen, J. M.; Johnson, K. R.; Wheelock, M. J. N-cadherin-catenin complexes form prior to cleavage of the proregion and transport to the plasma membrane. *J. Biol. Chem.* **2003**, *278* (19), 17269−17276.

(30) Yano, H.; Mazaki, Y.; Kurokawa, K.; Hanks, S. K.; Matsuda, M.; Sabe, H. Roles played by a subset of integrin signaling molecules in cadherin-based cell−cell adhesion. *J. Cell Biol.* **2004**, *166* (2), 283−295.

(31) Dionne, C. J.; Tse, K. Y.; Weiss, A. H.; Franco, C. B.; Wiest, D. L.; Anderson, M. K.; Rothenberg, E. V. Subversion of T lineage commitment by PU.1 in a clonal cell line system. *Dev. Biol.* **2005**, *280* (2), 448−466.

(32) Petrovick, M. S.; Hiebert, S. W.; Friedman, A. D.; Hetherington, C. J.; Tenen, D. G.; Zhang, D. Multiple functional domains of AML1: PU.1 and C/EBPα synergize with different regions of AML1. *Mol. Cell. Biol.* **1998**, *18* (7), 3915−3925.

(33) Hosokawa, H.; Ungerbäck, J.; Wang, X.; Matsumoto, M.; Nakayama, K. I.; Cohen, S. M.; Tanaka, T.; Rothenberg, E. V. Transcription factor PU.1 represses and activates gene expression in early T cells by redirecting partner transcription factor binding. *Immunity* **2018**, *48* (6), 1119−1134.

(34) Rothenberg, E. V.; Hosokawa, H.; Ungerbäck, J. Mechanisms of action of hematopoietic transcription factor PU.1 in initiation of T-cell development. *Front. Immunol.* **2019**, *10*, 228.

Proximity-dependent initiation of hybridization chain reaction. *Nat. Commun.* **2015**, *6*, 7294.

H

(35) Berx, G.; Roy, F. V. The E-cadherin/catenin complex: An important gatekeeper in breast cancer tumorigenesis and malignant progression. *Breast Cancer Res.* **2001**, *3* (5), 289.

(36) Karayiannakis, A. J.; Nakopoulou, L.; Gakiopoulou, H.; Keramopoulos, A.; Davaris, P. S.; Pignatelli, M. Expression patterns of β-catenin in in situ and invasive breast cancer. *Eur. J. Surg. Oncol. EJSO* **2001**, *27* (1), 31−36.

(37) Zadeh, J. N.; Steenberg, C. D.; Bois, J. S.; Wolfe, B. R.; Pierce, M. B.; Khan, A. R.; Dirks, R. M.; Pierce, N. A. NUPACK: Analysis and design of nucleic acid systems. *J. Comput. Chem.* **2011**, *32* (1), 170−173.

(38) Wolfe, B. R.; Porubsky, N. J.; Zadeh, J. N.; Dirks, R. M.; Pierce, N. A. Constrained multistate sequence design for nucleic acid reaction pathway engineering. *J. Am. Chem. Soc.* **2017**, *139*, 3134−3144.

(39) Cleary, B.; Simonton, B.; Bezney, J.; Murray, E.; Alam, S.; Sinha, A.; Habibi, E.; Marshall, J.; Lander, E. S.; Chen, F.; Regev, A. Compressed sensing for highly efficient imaging transcriptomics. *Nat. Biotechnol.* **2021**, *39*, 936−942.

(40) Janesick, A.; Scheibinger, M.; Benkafadar, N.; Kirti, S.; Ellwanger, D. C.; Heller, S. Cell-type identity of the avian cochlea. *Cell Rep* **2021**, *34* (12), 108900.

(41) Kim, M.-H.; Radaelli, C.; Thomsen, E. R.; Monet, D.; Chartrand, T.; Jorstad, N. L.; Mahoney, J. T.; Taormina, M. J.; Long, B.; Baker, K.; Bakken, T. E.; Campagnola, L.; Casper, T.; Clark, M.; Dee, N.; D'Orazi, F.; Gamlin, C.; Kalmbach, B. E.; Kebede, S.; Lee, B. R.; Ng, L.; Trinh, J.; Cobbs, C.; Gwinn, R. P.; Keene, C. D.; Ko, Andrew L; Ojemann, J. G.; Silbergeld, D. L.; Sorensen, S. A.; Berg, J.; Smith, K. A.; Nicovich, P. R.; Jarsky, T.; Zeng, H.; Ting, J. T.; Levi, B. P.; Lein, E. Target cell-specific synaptic dynamics of excitatory to inhibitory neuron connections in supragranular layers of human neocortex. *eLife* **2023**, *12*, No. e81863.

(42) Pavani, S. R. P.; Thompson, M. A.; Biteen, J. S.; Lord, S. J.; Liu, N.; Twieg, R. J.; Piestun, R.; Moerner, W. E. Three-dimensional, single-molecule fluorescence imaging beyond the diffraction limit by using a double-helix point spread function. *Proc. Natl. Acad. Sci. U. S. A.* **2009**, *106* (9), 2995−2999.

(43) Shtengel, G.; Galbraith, J. A.; Galbraith, C. G.; Lippincott-Schwartz, J.; Gillette, J. M.; Manley, S.; Sougrat, R.; Waterman, C. M.; Kanchanawong, P.; Davidson, M. W.; Fetter, R. D.; Hess, H. F. Interferometric fluorescent super-resolution microscopy resolves 3D cellular ultrastructure. *Proc. Natl. Acad. Sci. U. S. A.* **2009**, *106* (9), 3125−3130.

(44) Lee, J.; Stovall, G.; Ellington, A. Aptamer therapeutics advance. *Curr. Opin. Chem. Biol.* **2006**, *10* (3), 282−289.

(45) Tan, Y. H.; Liu, M.; Nolting, B.; Go, J. G.; Gervay-Hague, J.; Liu, G. A nanoengineering approach for investigation and regulation of protein immobilization. *ACS Nano* **2008**, *2* (11), 2374−2384.

(46) Pleiner, T.; Bates, M.; Görlich, D. A toolbox of anti-mouse and anti-rabbit IgG secondary nanobodies. *J. Cell Biol.* **2018**, *217* (3), 1143−1154.

(47) Alam, M. S. Proximity ligation assay (PLA). In *Immunohistochemistry and Immunocytochemistry: Methods and Protocols*; Methods in Molecular Biology; Springer, 2022; vol *2422*, pp 191−201.